An Improved Broadband Decoupling Sequence for Liquid Crystals and Solids

B. M. Fung, A. K. Khitrin,[1] and Konstantin Ermolaev[2]

Department of Chemistry and Biochemistry, University of Oklahoma, Norman, Oklahoma 73019-0370

Recently we developed an efficient broadband decoupling sequence called SPARC-16 for liquid crystals [*J. Magn. Reson.* 130, 317 (1998)]. The sequence is based upon a 16-step phase cycling of the 2-step TPPM decoupling method for solids [*J. Chem. Phys.* 103, 6951 (1995)]. Since then, we have found that a stepwise variation of the phase angle in the TPPM sequence offers even better results. The application of this new method to a liquid crystalline compound, 4-*n*-pentyl-4′-cyanobiphenyl, and a solid, L-tyrosine hydrochloride, is reported. The reason for the improvement is explained by an analysis of the problem in the rotating frame.   © 2000 Academic Press

Key Words: **broadband decoupling; liquid crystals; SPINAL-64.**

INTRODUCTION

The application of heteronuclear broadband decoupling is essential for the observation of high-resolution NMR signals of ^{13}C and other spin-1/2 nuclei, whether the sample is in liquid, liquid crystalline, or solid state. Many efficient broadband decoupling sequences for liquid, such as MLEV (*1–4*), WALTZ (*5, 6*), and GARP (*7, 8*), are based on the use of composite pulses with systematic phase cycling. In principle, the more efficient adiabatic frequency-sweeping method developed recently (*9–17*) does not depend on phase shifting, but in practical implementation the frequency sweep is often accomplished by programmed phase shifts using a fixed radiofrequency (RF) source. The most efficient broadband decoupling method for solids reported so far is a 2-step phase shifting scheme called TPPM (two pulse phase-modulation; *18*). We have shown that the TPPM sequence also works well for liquid crystals (*19*), and its performance is better than that of all the previously published broadband decoupling sequences (*6–9, 20–25*). Furthermore, the decoupling efficiency is improved by incorporating the TPPM scheme into a supercycle called SPARC-16, with is an abbreviation for small phase angle rapid cycling with 16 steps (*19*). Since then, we have found that a stepwise change in the phase angle of the TPPM sequence, combined with overall phase cycling, offers even

better results for broadband decoupling for liquid crystals and solids. The method is called SPINAL-64, an acronym for small phase incremental alternation, with 64 steps, and the results are discussed in the following pages.

RESULTS AND DISCUSSION

The TPPM (*18*) and SPARC-16 (*19*) decoupling sequences are continuous cycles composed of two pulses P and $\bar{\text{P}}$ with opposite phases, where P = 165(10°) and $\bar{\text{P}}$ = 165(−10°):

$$\text{TPPM} = \text{P}\bar{\text{P}}$$

$$\text{SPARC-16} = \text{P}\bar{\text{P}}\bar{\text{P}}\text{P}\ \bar{\text{P}}\text{PP}\bar{\text{P}}\ \text{PP}\bar{\text{P}}\text{P}\ \bar{\text{P}}\bar{\text{P}}\text{P}\bar{\text{P}}.$$

The actual pulse width can be slightly different from 165° and the actual phase shift can be slightly different from ±10° without appreciable deleterious effect on the performance.

In further studies, we have found that changing the phase angles in the basic elements P and $\bar{\text{P}}$ stepwise actually leads to considerable improvement in the efficiency of broadband decoupling for liquid crystals. Thus, two basic elements are constructed in the following way:

$$Q = 165(10°)\ 165(−10°)\ 165(15°)\ 165(−15°)$$
$$\times\ 165(20°)\ 165(−20°)\ 165(15°)\ 165(−15°)$$

and

$$\bar{Q} = 165(−10°)\ 165(10°)\ 165(−15°)\ 165(15°)$$
$$\times\ 165(−20°)\ 165(20°)\ 165(−15°)\ 165(15°).$$

These elements are then combined into supercycles, and the sequences are called SPINAL:

$$\text{SPINAL-16} = Q\bar{Q}$$

$$\text{SPINAL-32} = Q\bar{Q}\bar{Q}Q$$

$$\text{SPINAL-64} = Q\bar{Q}\bar{Q}Q\ \bar{Q}QQ\bar{Q}$$

$$\text{SPINAL-128} = Q\bar{Q}\bar{Q}Q\ \bar{Q}QQ\bar{Q}\ QQ\bar{Q}Q\ \bar{Q}\bar{Q}Q\bar{Q}.$$

FIG. 1. ^{13}C-NMR spectra of 4-n-pentyl-4′-cyanobiphenyl (5CB) at 9.4 T and ambient temperature. The decoupling power ($\gamma B_2/2\pi$) was 18 kHz. The decoupling sequences were (a) WALTZ-16; (b) TPPM; (c) SPARC-16; and (d) SPINAL-64. The peak assignment is (from left to right for decreasing chemical shifts): 4, 1′, 1, 4′, 3′, 3, 2′, 2, γ, α, β, δ, ω, and −CN (The assignment of the γ and α peaks were reversed in *19*).

To compare the efficiencies of different broadband decoupling sequences, we chose to study the ^{13}C NMR spectra of the benchmark liquid crystal, 4-n-pentyl-4′-cyanobiphenyl (5CB), which has the following structure.
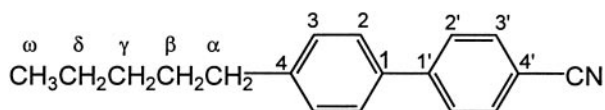
Figure 1 shows the results of applying the broadband decoupling sequences TPPM, SPARC-16, and SPINAL-64 on the ^{13}C spectra of 5CB. The WALTZ-16 sequence (*5, 6*) is also chosen for comparison because it is very efficient for broadband decoupling of liquid samples and widely used. However,

it is not designed for systems with dipolar couplings and the ^{13}C linewidths are considerably larger than those obtained from using the other three sequences. Unfortunately, some investigators are unaware of this and use WALTZ-16 decoupling for liquid crystal samples, requiring much higher proton decoupler power to obtained resolved peaks. Even with considerably higher decoupler power, the observed ^{13}C peaks are often much broader because RF heating would create an undesirable temperature gradient in the sample (*26*).

Because the TPPM sequence does not compensate for the effect of proton chemical shift differences, the linewidths of different ^{13}C peaks in a spectrum vary with the proton decoupler frequency differently. The SPINAL-64 sequence suffers from the same problem. For example, when the proton decoupling frequency is moved to the direction of the aliphatic part of the spectrum, the widths of four of the five aliphatic ^{13}C peaks increase, but that of the α carbon decreases (Fig. 2). Thus, the peaks of the α and β carbons overlap in Fig. 2Ic, when TPPM decoupling is used, but they are still sufficiently
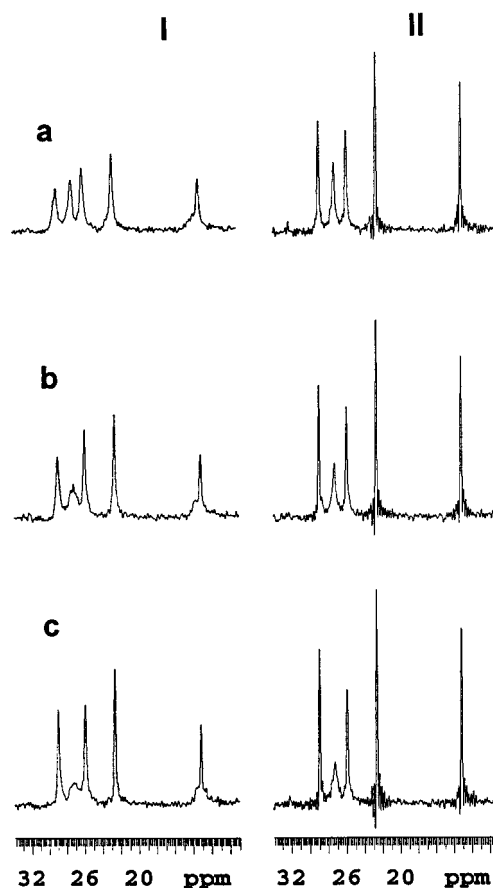
FIG. 2. ^{13}C-NMR spectra of 4-n-pentyl-4′-cyanobiphenyl (5CB) at 9.4 T and ambient temperature. Only the peaks of the aliphatic carbons are shown. The decoupling power ($\gamma B_2/2\pi$) was 18 kHz. The relative offsets of the decoupler were (a) 0 Hz; (b) 100 Hz; and (c) 200 Hz; toward the aliphatic region of the proton spectrum. Column I: TPPM decoupling; column II: SPINAL-64 decoupling.

resolved with SPINAL-64 decoupling (Fig. 2IIc). In the mean time, the aromatic peaks are less affected by small changes in the proton decoupler frequency (spectra not shown).

The spectra in Figs. 1 and 2 clearly show that the SPINAL-64 sequence performs much better than TPPM and SPARC-16. The SPARC-16 sequences use permutations of the basic element P and P̄ in TPPM to form a supercycle and achieve better results (*19*), but the improvement is small. On the other hand, by changing the phase angle stepwise to form two basic cycles Q and Q̄ and then combining them into a supercycle, SPINAL-64 gives a much better performance. Its application to many other liquid crystals gave similar results. In fact, the linewidths of the δ and ω carbons in 5CB are so narrow that they show a ringing pattern due to truncation of the free induction decay with a 40-ms acquisition time (Fig. 2, column II).

The decoupling efficiency of SPINAL-64 for solids is also better than that of TPPM, which is in turn better than continuous wave (CW) decoupling. The results obtained for L-tyrosine hydrochloride with magic angle spinning (MAS) are shown in Fig. 3. Although the improvement is less than that for liquid crystals (Figs. 1 and 2), it is still quite significant.

The theoretical basis for TPPM decoupling was analyzed by using a three-spin system, a CH_2 group (*18*). A detailed theoretical analysis of a many-spin system, such as 5CB, is extremely difficult if not impossible. This point is underscored by considering the different dependence of the linewidths of different carbons on the decoupler frequency (Fig. 2), as discussed above. However, a qualitative analysis is feasible. The following explanation is presented to help understand why, for liquid crystals, the performance of the SPINAL-64 sequence is much better than that of the TPPM pulse sequence.

The Hamiltonian in the rotating frame for the protons (I) and the ^{13}C spins (S) is

$$\mathscr{H} = \mathscr{H}_{RF} + \sum_{j>0} \delta_j I_{jz} + \mathscr{H}_{IS} + \mathscr{H}_{II}, \qquad [1]$$

where $\mathscr{H}_{RF}$ is the interaction of the spin system with the RF decoupling pulses, δ_j accounts for the chemical shift of the $j$the spin measured from the decoupler frequency, and $\mathscr{H}_{IS}$ and $\mathscr{H}_{II}$ are the dipole–dipole interactions between a single ^{13}C spin and surrounding protons, and between the proton spins, respectively;

$$\mathscr{H}_{IS} = \sum_{j>0} 2 \, b_{0j} \, S_{0z} I_{jz},$$

$$\mathscr{H}_{II} = \sum_{i>j>0} b_{ij}(2 \, I_{iz} I_{jz} - I_{ix} I_{jx} - I_{iy} I_{jy}), \qquad [2]$$

b_{ij} being the constants of the dipole–dipole interaction. The chemical shift terms of the S spins and the I-I and I-S scalar couplings are omitted for the sake of simplicity. For the TPPM

and SPINAL sequences, the phases of the RF pulses $\Phi(t)$ are small. Therefore, up to first order in Φ, the RF field interaction term (in angular frequency units) can be written as

$$\mathscr{H}_{RF} = -\omega_{RF}[I_x + \Phi(t)I_y], \qquad [3]$$

where $\omega_{RF} = \gamma B_{RF}$ is the amplitude of the decoupling field, and I_x and I_y are the components of the total proton magnetization along the x and y axes of the rotating frame, respectively. As an example, the phase function for TPPM sequence is

$$\Phi(t) = \begin{cases} \pi/18, & 2k\tau < t < (2k+1)\tau \\ -\pi/18, & (2k+1)\tau < t < (2k+2)\tau \end{cases}, \qquad [4]$$

where $k = 0, 1, 2, \ldots$, and τ is the length of the pulses.

Each proton spin j experiences an influence of its own effective RF field ω_j with the components ω_{RF} and δ_j. It is convenient to use a tilted frame with the x axis for each proton spin aligned along its effective RF field and retain only the secular parts of the dipolar interactions with respect to the major interaction $\sum \omega_j \cdot I_j$. A transformation to this frame is accomplished by a rotation in the operator space of each proton spin at the angle $\varphi_j = \arctan(\delta_j/\omega_{RF})$ around the y axis. The effective Hamiltonian in this frame is

$$\mathscr{H}_{eff} = -\sum_{j>0} |\omega_j| I_{jx} - \omega_{RF} \Phi(t) I_y \qquad [5]$$
$$+ \sum_{j>0} 2 \, (\delta_j/|\omega_j|) b_{0j} S_{0z} I_{jx} + \mathscr{H}_{IIsec},$$

where $|\omega_j| = (\omega_{RF}^2 + \delta_j^2)^{1/2}$ and $\mathscr{H}_{IIsec}$ is the secular part of the homonuclear dipolar interaction (for $\delta_j \equiv 0$ it becomes $-(1/2)\mathscr{H}_{dx}$, where $\mathscr{H}_{dx}$ is the secular part of the dipolar interaction between protons with respect to the x axis).

For $\Phi(t) = 0$ (cw decoupling), the third term in Eq. [5] on the right-hand side represents the residual heteronuclear coupling and gives the main contribution to the ^{13}C linewidth. Resonant harmonics of $\Phi(t)$ cause a resonance in the rotating frame, leading to flips of the x-components of the proton spins and averaging out the residual heteronuclear interaction. There are three main factors that broaden the resonance in the rotating frame and make the decoupling less efficient: distribution of the proton chemical shifts, RF field inhomogeneity, and homonuclear dipolar interactions. The first two create an inhomogeneous distribution of the resonance frequencies $|\omega_j|$. In liquid crystals, there is only a finite number of large intramolecular contributions to the homonuclear dipolar Hamiltonian, nonaveraged by the molecular motions. Although individual lines are usually not resolved in the dipolar spectrum, the spectrum has some features of an inhomogeneous system and shows numerous peaks with acquisition delay (*27*). Therefore, it presents an intermediate case between homogeneous and inhomogeneous broadening.
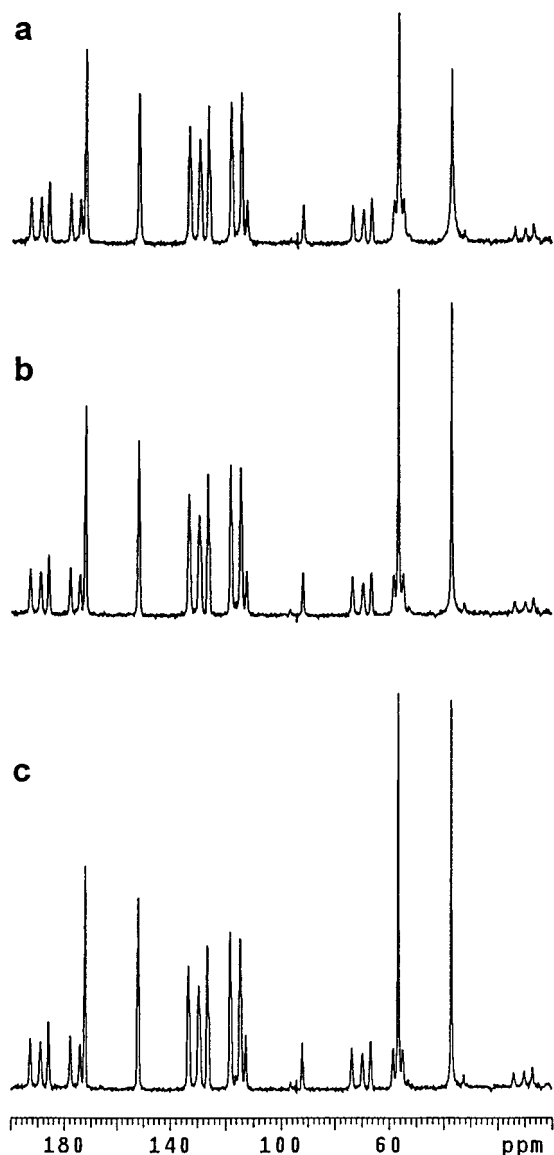
FIG. 3. ^{13}C-NMR spectra of L-tyrosine hydrochloride at 9.4 T and ambient temperature. The MAS rate was 6 kHz and the decoupling power ($\gamma B_2/2\pi$) was 75 kHz. Sideband elimination technique was not used to avoid possible intensity distortion. The number of scans was 100 for each spectrum, and no line broadening was used for data processing. The assignment of the center-band peaks is (from left to right for decreasing chemical shifts): –COOH, ζ, δ, δ', γ, ϵ, ϵ', α, and β. (a) CW decoupling; (b) TPPM decoupling; (c) SPINAL-64 decoupling.

Figure 4a shows a spectrum of $\Phi(t)$ (modulus of the Fourier coefficients) for the TPPM sequence. The frequency is in the units of ω_{RF}, the resonance frequency in the rotating frame in the absence of broadening factors mentioned above. In the range displayed, it has only one peak at the frequency π/τ (or $\pi/(\omega_{RF}\tau)$ in the dimensionless units of Fig. 4), where τ is the pulse width. The proton chemical shifts increase the resonance frequencies in the rotating frame and shift the center of the absorption line to higher frequencies. Therefore, the best per-

formance is achieved at pulse angles ($\omega_{RF}\tau$) shorter than π (165° in our case).

As it was mentioned above, the absorption spectrum in the rotating frame is highly inhomogeneous, and it is difficult to saturate it by irradiating at a single frequency. Much better results can be achieved when the function $\Phi(t)$ has more harmonics in the resonance region, as for the SPINAL-32 pulse sequence shown in Fig. 4b. The number of harmonics of the SPINAL-64 sequence further increases, and the corresponding spectrum of excitation in the rotating frame is displayed in Fig. 4c.

In practice, the performance of SPINAL-64 was only slightly better than that of SPINAL-32, and no further improvement was observed for SPINAL-128, which has even more harmonics. There are two likely reasons for this. First, for a fixed decoupler power, an increase in frequency dispersion reduces the intensity of each component of the harmonics. Second, the ^{13}C signals of liquid crystals have fairly small T_2's, making the very long SPINAL-128 sequence no more advantageous than SPINAL-64. Many other values of phase shifts were tested, but they were not as good as the basic cycles Q and $\bar{Q}$ shown above.

In summary, new broadband decoupling sequences have been designed by changing the phase angles in the TPPM sequence stepwise and then combining the basic cycles into supercycles. It has been shown that SPINAL-64 sequence performs much better than other sequences for the broadband decoupling of liquid crystals and solids. The reason for the improvement is explained by an analysis of the problem in the rotating frame. Based upon this analysis, it is possible to
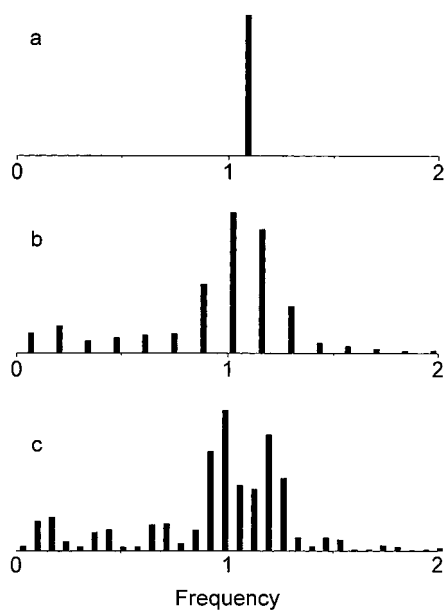

FIG. 4. Irradiation "spectra" in the rotating frame for the pulse sequences (a) TPPM; (b) SPINAL-32; and (c) SPINAL-64. The frequency is in units of ω_{RF}.

construct other decoupling sequences with even better performance. The results will be reported elsewhere.

EXPERIMENTAL

All the experiments were carried out on a Varian UNITY/INOVA 400 MHz NMR spectrometer equipped with a waveform generator for generating decoupling sequences. The liquid crystal experiments were performed at ambient temperature using an indirect detection probe manufactured by Narolac Corporation (Martinez, CA). To minimize RF heating, a very small duty cycle (1%) was used, with an overall cycling time of 5 s (0.01 s preacquisition irradiation for NOE effect, 0.04 s acquisition time, and 4.95 s relaxation delay). Single-pulse rather than cross polarization was used to show proper intensities for the quaternary and cyano carbons. A Varian probe was used for the MAS experiment; the cross polarization time was 4 ms, the acquisition time was 0.03 ms, and the cycling time was 10 s.

ACKNOWLEDGMENT

REFERENCES

1. M. H. Levitt and R. Freeman, *J. Magn. Reson.* **43**, 502 (1981).
2. M. H. Levitt, R. Freeman, and T. Frenkiel, *J. Magn. Reson.* **47**, 328 (1982).
3. M. H. Levitt, R. Freeman, and T. Frenkiel, *J. Magn. Reson.* **50**, 157 (1982).
4. M. H. Levitt, R. Freeman, and T. Frenkiel, *in* "Advances in Magnetic Resonance" (J. S. Waugh, Ed.), Vol. 11, p. 47, Academic Press, New York (1983).
5. A. J. Shaka, J. Keeler, T. Frenkiel, and R. Freeman, *J. Magn. Reson.* **52**, 335 (1983).
6. A. J. Shaka, J. Keeler, and R. Freeman, *J. Magn. Reson.* **53**, 313 (1983).
7. A. J. Shaka, P. B. Barker, and R. Freeman, *J. Magn. Reson.* **64**, 547 (1985).
8. A. J. Shaka and J. Keeler, *Prog. NMR Spectrosc.* **19**, 47 (1987).
9. Z. Starcuk, Jr., K. Bartusek, and Z. Starcuk, *J. Magn. Reson. A* **107**, 24 (1994).
10. T. E. Skinner and M. R. Bendall, *J. Magn. Reson. A* **112**, 126 (1995).
11. E. Kupce and R. Freeman, *J. Magn. Reson. A* **115**, 273 (1995).
12. E. Kupce and R. Freeman, *J. Magn. Reson. A* **117**, 246 (1995).
13. E. Kupce and R. Freeman, *Chem. Phys. Lett.* **250**, 523 (1996).
14. E. Kupce and R. Freeman, *J. Magn. Reson. A* **118**, 299 (1996).
15. R. Fu and G. Bodenhausen, *Chem. Phys. Lett.* **245**, 415 (1995).
16. R. Fu and G. Bodenhausen, *J. Magn. Reson. A* **117**, 324 (1995).
17. R. Fu and G. Bodenhausen, *J. Magn. Reson. A* **119**, 129 (1996).
18. A. E. Bennett, C. M. Rienstra, M. Auger, K. V. Lakshmi, and R. G. Griffin, *J. Chem. Phys.* **103**, 6951 (1995).
19. Y. Yu and B. M. Fung, *J. Magn. Reson.* **130**, 317 (1998).
20. J. S. Waugh, *J. Magn. Reson.* **49**, 517 (1982).
21. B. M. Fung, D. S. L. Mui, I. R. Bonnell, and E. L. Enwall, *J. Magn. Reson.* **58**, 254 (1984).
22. D. Suter, K. V. Schenker, and A. Pines, *J. Magn. Reson.* **73**, 90 (1987).
23. K. V. Schenker, D. Suter, and A. Pines, *J. Magn. Reson.* **73**, 99 (1987).
24. D. Suter, A. Pines, J. H. Lee, and G. Drobny, *Chem. Phys. Lett.* **144**, 324 (1988).
25. J. J. Kotyk and J. R. Garbow, *J. Magn. Reson.* **89**, 647 (1990).
26. B. M. Fung, *J. Magn. Reson.* **86**, 160 (1990).
27. Y. Yu and B. M. Fung, *Mol. Phys.* **94**, 863 (1998).